SVN Stroke & Vascular Neurology

Prominent juxtacortical white matter lesion hallmarks *NOTCH3*-related intracerebral haemorrhage

Chih-Hao Chen ,[1] Hao-Chia Hsu,[2] Yu-Wen Cheng,[3] Ya-Fang Chen,[4] Sung-Chun Tang,[2] Jiann-Shing Jeng[1]

To cite: Chen C-H, Hsu H-C, Cheng Y-W, *et al*. Prominent juxtacortical white matter lesion hallmarks *NOTCH3*-related intracerebral haemorrhage. *Stroke & Vascular Neurology* 2022;**7**: e001020. doi:10.1136/svn-2021-001020

Received 24 March 2021
Accepted 11 July 2021
Published Online First 3 August 2021

[1]Neurology, National Taiwan University Hospital, Taipei, Taiwan
[2]Department of Neurology, National Taiwan University Hospital, Taipei, Taiwan
[3]Department of Neurology, National Taiwan University Hospital Hsinchu Branch, Hsinchu, Taiwan
[4]Medical Imaging, National Taiwan University Hospital, Taipei, Taiwan

Correspondence to
Dr Sung-Chun Tang; tangneuro@gmail.com

Dr Ya-Fang Chen; joannayfc@gmail.com

ABSTRACT

Background and purpose *NOTCH3* p.R544C mutation accounts for 5% of spontaneous intracerebral haemorrhage (ICH) in East Asian patients. We investigated whether certain CT features are associated with *NOTCH3*-related ICH.

Methods Patients with spontaneous ICH from a prospective stroke registry were screened for *NOTCH3* p.R544C mutation. The neuroimaging features on the initial non-contrast CT scans selected to predict *NOTCH3* p.R544C mutation, including burden of white matter lesion (WML), degree of brain atrophy, number of lacunes, prominent juxtacortical WML and prominent lobar lacunes, were analysed by neuroradiologists blinded to the mutation status.

Results Of 299 patients with spontaneous ICH (mean age, 61 years; male, 68%; ICH volumes, 14.1±17.8 mL), 13 patients (4.3%) carried *NOTCH3* p.R544C mutation. The clinical features, haematoma size and location were similar between *NOTCH3* p.R544C mutation carriers and non-carriers. The CT scan revealed that patients with *NOTCH3* p.R544C mutation had more severe WML and more frequently had prominent juxtacortical WML (69.2% vs 17.8%, p<0.001), and the effects were not driven by ageing as seen in patients without mutation. Prominent juxtacortical WML (area under receiver operating characteristic curve=0.76) outperformed the total WML score and prominent lobar lacunes and significantly predicted *NOTCH3* p.R544C mutation in a multivariable-adjusted model (OR, 20.9; 95% CI 4.94 to 88.6).

Conclusion In patients with spontaneous ICH, the severity and topographic distribution of WML can help in identifying potential *NOTCH3* mutation-related ICH.

INTRODUCTION

Intracerebral haemorrhage (ICH) accounts for 10%–15% of all stroke cases and is associated with a high risk of morbidity and mortality.[1] The two major causes of spontaneous ICH are hypertensive angiopathy and cerebral amyloid angiopathy, both belonging to the spectrum of cerebral small vessel disease (SVD).[2 3] In addition to these two acquired SVDs, cerebral autosomal dominant arteriopathy with subcortical infarcts and leukoencephalopathy (CADASIL), caused by the cysteine-altering mutation of *NOTCH3*, is the most common hereditary cause of cerebral SVD.[4] Patients with CADASIL usually experience migraine, repeated ischaemic stroke and progressive gait and cognitive decline.[5] In addition to subcortical infarcts, patients with CADASIL may develop ICH, particularly in East Asian patients.[6 7]

In Taiwan, a hot spot mutation at exon 11 p.R544C of *NOTCH3* accounts for >70% of patients with CADASIL.[8 9] One study reported that up to 40% of patients with CADASIL in Taiwan harbouring *NOTCH3* p.R544C mutation may experience ICH during their lifetime, and those with ICH as their first stroke event had significantly higher risks of recurrent stroke and mortality.[6] Screening patients from a multicentre stroke registry in Taiwan showed that *NOTCH3* p.R544C mutations were found in up to 5% of all patients with spontaneous ICH.[10]

As *NOTCH3* mutation is present in a certain number of patients with spontaneous ICH, they must be identified earlier to perform a comprehensive evaluation of the patient and to provide genetic counselling to their family members. Whether certain diagnostic features can distinguish *NOTCH3* mutation-related ICH remained unknown. Patients with ICH usually receive CT as the first-line neuroimaging study. A CT-based feature selection method to screen patients potentially harbouring *NOTCH3* mutation can be practical and has great value in a clinical setting. Therefore, we investigate whether distinct CT features in patients with ICH are associated with the *NOTCH3* mutation.

METHODS

Participants

This study was approved by the research ethics committees of the participating hospital. Written informed consent was obtained from all patients and/or their relatives. The data of this study are available from the corresponding author on reasonable request. The study protocol was conducted in accordance

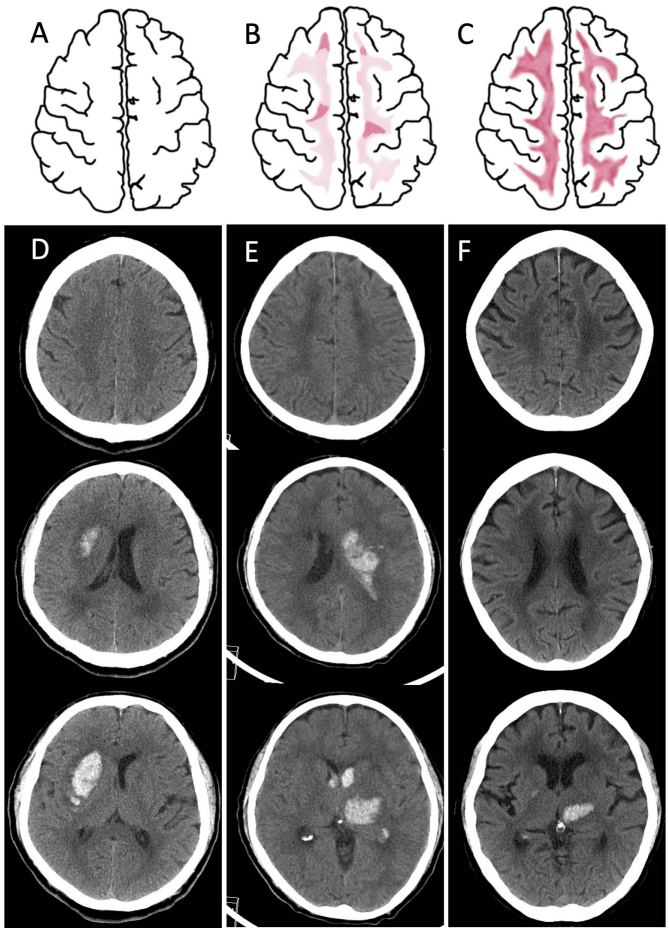

Figure 1 Schematic and neuroimaging demonstration of prominent juxtacortical WML. (A–C) Schematic diagrams of the WML at the level of CS. (A) A normal CS without WML. (B) Pattern 1: bilateral vague hypodensity change in CS with patchy areas of low densities inside, involving the juxtacortical region. (C) Pattern 2: bilateral diffuse hypodensity change in CS, extending to the juxtacortical region, delineating a sharp interface of grey–white matter junction. (D–F) CT scans of 3 different patients of ICH. (D) A case of right putaminal haemorrhage with negative *NOTCH3* p.R544C mutation was scored 1 and 2 for frontal and parietal lobe WML but without WML in the CS. (E) A case of left thalamic haemorrhage with positive *NOTCH3* p.R544C mutation, was scored 2 for frontal and parietal lobe WML, with pattern 1 change in CS. (F) A case of left thalamic haemorrhage with positive *NOTCH3* p.R544C mutation was scored 2 for frontal and parietal lobe WML, with pattern 2 change in the CS. Note that the ventricular-level white matter also reveals extensive WML reaching the grey–white matter interface. CS, centrum semiovale; ICH, intracerebral haemorrhage; WML, white matter lesion.

with the Formosan Stroke Genetic Consortium (FSGC), and the detailed methodology was published elsewhere.[10] Briefly, patients with acute stroke within 10 days of onset and with available neuroimaging data were recruited. Only patients who presented with acute ICH were included in the present study. Genomic DNA was extracted from peripheral blood, and *NOTCH3* mutation p.R544C was genotyped through PCR and subsequently confirmed through DNA sequencing. Information regarding clinical features was collected including vascular risk factors (such as hypertension, diabetes mellitus, hyperlipidemia and smoking status), family history of stroke, initial stroke severity (assessed using the National Institute of Health Stroke Scale), ICH score (a 6-point score consisting of age, ICH volume, initial Glasgow Coma Scale, presence of intraventricular haemorrhage and infratentorial origin of bleeding to predict 30-day mortality),[11] length of stay during hospitalisation and functional status at discharge (assessed using Barthel's Index and the modified Rankin Scale).

Neuroimaging features

The initial non-contrast CT scans were immediately performed after patients' index ICH events with a standard slice thickness of 5 mm. The ICH volume was calculated based on the $(a \times b \times c)/2$ formula, where a and b represented the largest perpendicular diameters of the ICH and c represented the number of CT slices with haematoma multiplied by the slice thickness.[12] The locations of ICH were classified into basal ganglia, thalamus, cortical–subcortical, infratentorium and multiple locations.

Neuroimaging features of SVD based on non-contrast CT included the severity of white matter lesion (WML), cerebral atrophy and lacunes. WML was the area with ill-defined hypodensity (compared with the normal-appearing white matter) in the periventricular or subcortical regions. WML severity was assessed using a visual rating scale proposed by van Sweiten *et al*.[13] In brief, WML was graded in the anterior (region around the anterior horn of the lateral ventricle) and posterior (region around the posterior horn of the lateral ventricle and centrum semiovale (CS)) parts separately. A score of 1 indicated WML restricted to the periventricular region, whereas a score of 2 indicated the hypodensity involved in the subcortical region. The summation of anterior and posterior WML scores resulted in an overall WML score of 0 to 4. Since CADASIL was known for the WML in the anterior temporal lobe and external capsule, we further recorded whether hypodensity existed in the anterior temporal lobe and external capsule on the CT scans. Of note, the hypodensity in the external capsule area that could be attributed to dilated perivascular space or old insults related were not included.

In addition, we defined a sign of prominent juxtacortical WML which can be evaluated at the CS level (1 cm or 2 slices above the lateral ventricular roof; figure 1A–C). The prominent juxtacortical WML we proposed here suggested a more severe WML toward the periphery of the white matter than that defined in the grading system reported by van Sweiten *et al*.[13] Patients with higher WML scores but no prominent juxtacortical WML usually showed ill-defined periventricular hypodensities that spread out gradually and fused with the normal-appearing whiter matter without a clear border (figure 1D). Prominent juxtacortical WML included two patterns, either

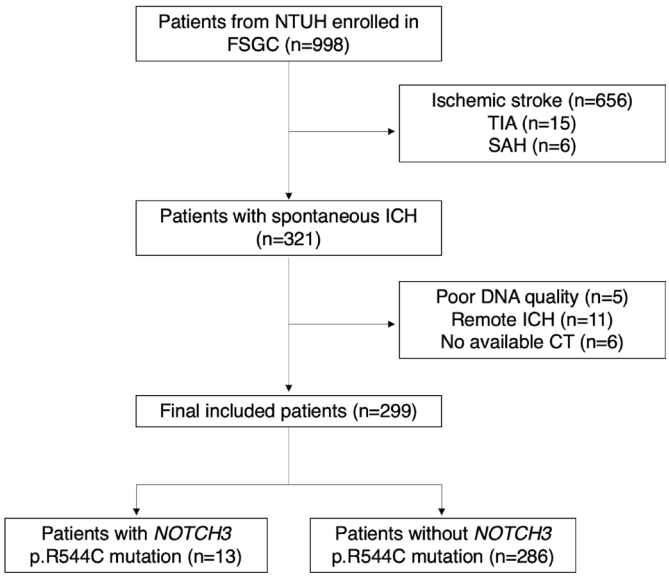

Figure 2 Flowchart of participant recruitment. FSGC, Formosan Stroke Genetic Consortium; ICH, intracerebral haemorrhage; NTUH, National Taiwan University Hospital; SAH, subarachnoid haemorrhage; TIA, transient ischaemic attack.

(1) bilateral vague hypodensity of the CS with nodular or patchy areas of low densities inside, involving the juxtacortical region (figure 1E) or (2) bilateral diffuse hypodensities of the CS, extending to the juxtacortical region, delineating a sharp interface of grey–white matter junction (figure 1F). The pattern 1 is milder, with inhomogeneous low density of the CS. The pattern 2 reflects a very severe WML reaching the juxtacortical region, which usually can also be seen at the ventricular level.

The degree of cerebral atrophy was adapted from a visual rating scale described by Sato *et al*.[14] Atrophy severity was assessed at the central (deep nucleus and lateral ventricle level) and cortical (supraventricular or CS level) areas, with scores of 0 (no atrophy), 1 (modest atrophy) and 2 (severe atrophy), leading to a total atrophy score of 0 to 4. In patients with supratentorial ICH, the WML degree and cerebral atrophy were evaluated on the hemisphere contralateral to ICH. For those with infratentorial ICH, the hemisphere with more severe WML or atrophy was scored.

Lacune was defined as an ovoid or round cavity with a size of 3–15 mm in diameter with radiolucency similar to the cerebrospinal fluid. The presence and number of lacunes were documented after careful reviewing of CT in three orthogonal planes if reconstructed images were available (although in 53 cases, only the axial plane was available). A prominent lobar lacune was recorded if the patient had more lacunes in the cerebral white matter than in the deep nuclei or brain stem.

All the aforementioned SVD features were primarily assessed by an experienced neuroradiologist who was blinded to the patients' status of *NOTCH3* p.R544C mutation. The results were independently reviewed by another neurologist. The inter-rater agreement, expressed using weighted Kappa values, was 0.72 (95% CI 0.59 to 0.85) for the total WML score, 0.76 (95% CI 0.65 to 0.86) for the total atrophy score and 0.88 (95% CI 0.72 to 1.00) for prominent juxtacortical WML.

Part of the enrolled patients had received follow-up brain MRI, which was not mandatory but may help in clarifying the aetiology and severity of SVD. The aforementioned neuroimaging features on CT, except for the cerebral atrophy score, were all reviewed by MRI again to evaluate its consistency. The inter-rater agreement of Kappa value was 0.77 (0.60–0.94) for severe WML and 0.87 (0.74–1.00) for prominent juxtacortical WML.

Statistical analysis

Demographic and neuroimaging variables were compared between patients with and without *NOTCH3* p.R544C mutation by using the Mann-Whitney U test or Fisher's exact test as appropriate. The frequency of neuroimaging features distributed across different age groups between patients with and without *NOTCH3* p.R544C mutation was compared using the Cochrane-Mantel-Haenszel test. Logistic regression analysis was applied to test the independent association between *NOTCH3* p.R544C mutation and neuroimaging features. An unadjusted univariable regression was first applied, followed by covariate adjustment encompassing demographic features of age, sex and hyperlipidemia (which were also significant in univariable regression). Three CT features most relevant to *NOTCH3* p.R544C mutation (namely, the total WML score, prominent juxtacortical WML and prominent lobar lacune) were used in a multivariable regression model and the area under the receiver operating characteristic curve (AUC) was estimated to explore the ability of individual and combined neuroimaging features in predicting *NOTCH3* p.R544C mutation. Given the rare outcome of the dependent variable (*NOTCH3* p.R544C mutation), a penalised maximal likelihood approach was applied in the logistic regression process.[15] Besides, the agreement of neuroimaging features between CT and MRI in patients who had received MRI was measured by Cohen's Kappa values. All statistical analyses were performed using SAS V.9.4 (SAS Institute, Cary, North Carolina), and $p<0.05$ was considered statistically significant.

RESULTS

In total, 998 patients were enrolled in the FSGC, and 321 of them were diagnosed as having ICH. Of them, 299 patients (mean age, 61.4±14.7 years; men, 67.6%; ICH volume, 14.1±17.8 mL and ICH score, 1.14±1.04) had CT scan data available at the stroke onset. The study flowchart is shown in figure 2. Of 299 patients, 13 (4.3%) carried *NOTCH3* p.R544C mutation. Demographic features, stroke severity and discharge status were comparable between *NOTCH3* p.R544C mutation carriers and non-carriers, except that mutation carriers had a higher

Table 1 Clinical characteristics between patients with ICH with and without *NOTCH3* p.R544C mutation

	NOTCH3 mutation (–) n=286	*NOTCH3* mutation (+) n=13	P value
Age	61.3±14.7	64.2±12.1	0.44
Male sex	194 (67.8%)	8 (61.5%)	0.64
Medical history			
Hypertension	263 (92.0%)	11 (84.6%)	0.30
Diabetes mellitus	88 (31.0%)	5 (38.5%)	0.55
Hyperlipidaemia	89 (31.1%)	9 (69.2%)	**0.004**
Smoking	104 (36.6%)	3 (23.1%)	0.39
Heart disease	68 (23.9%)	1 (7.7%)	0.31
Previous ischaemic stroke	29 (10.1%)	2 (15.4%)	0.65
Previous ICH	27 (9.4%)	3 (23.1%)	0.16
Parental stroke	72 (25.4%)	4 (30.8%)	0.75
Sibling stroke	37 (13.1%)	4 (30.8%)	0.09
ICH location			0.39
Thalamus	77 (26.9%)	6 (46.2%)	
Basal ganglia	106 (37.1%)	3 (23.1%)	
Cortical-subcortical	55 (19.2%)	1 (7.7%)	
Infratentorium	46 (16.1%)	3 (23.1%)	
Multiple or others	2 (1.0%)	0 (0%)	
ICH size, mL	14.2±17.9	13.4±17.6	0.30
IVH	90 (31.7%)	4 (30.8%)	0.99
Admission status			
Glasgow coma scale	12.6±3.5	13.0±3.2	0.58
Systolic blood pressure	182.7±37.8	185.0±29.9	0.76
Diastolic blood pressure	101.7±25.0	100.5±14.2	0.96
Heart rate	86.3±17.8	86.0±23.2	0.36
NIHSS	13.0±9.5	13.1±11.5	0.77
ICH score	1.2±1.2	1.2±1.1	0.96
Discharge status			
Length of stay, days	15.5±14.4	10.9±5.7	0.48
NIHSS at discharge	10.1±11.6	13.8±14.0	0.37
Change of NIHSS	–3.3±8.3	0.7±7.1	**0.02**
Barthel index	59.6±36.8	39.2±44.9	0.13
Modified Rankin scale	2.9±1.6	3.5±1.9	0.20

Numbers in bold indicating statistical significance (P<0.05).
ICH, intracerebral haemorrhage; IVH, intraventricular haemorrhage; NIHSS, National Institute of Health Stroke Scale.

prevalence of hyperlipidemia (69% vs 31%, p=0.004; table 1). The most common ICH location in *NOTCH3* p.R544C mutation carriers was thalamus (46%), followed by the basal ganglia (23%) and infratentorium (23%). In *NOTCH3* p.R544C mutation non-carriers, the most frequency ICH locations were the basal ganglia (37%), thalamus (27%) and cortical–subcortical regions (19%).

Continuous variables were expressed as mean±SD and compared by Mann-Whitney U test; categorical variables were compared by Fisher's exact test.

Table 2 shows the CT features of SVD. Patients with *NOTCH3* p.R544C mutation had higher WML scores (2.8±1.7 vs 1.6±1.5, p=0.02) and were more likely to have external capsule WML involvement (46% vs 12%, p<0.001) and prominent juxtacortical WML (69% vs 16%, p<0.001). Two patients with *NOTCH3* p.R544C mutation having either pattern 1 (figure 1E) or pattern 2 (figure 1F) of prominent juxtacortical WML are shown. However, the proportion of pattern 1 versus 2 in patients with and without *NOTCH3* p.R544C mutation was comparable (p=0.72). Furthermore, the severity of cerebral atrophy and the presence of lacunes were also similar, although patients with *NOTCH3* p.R544C mutation had a non-significantly higher number of lacunes (1.9±2.1 vs

Table 2 CT features distinguishing patients with ICH with and without *NOTCH3* p.R544C mutation

	NOTCH3 mutation (–), n=286	*NOTCH3* mutation (+), n=13	P value	Unadjusted OR (95% CI)	Demographic-adjusted OR (95% CI)*
Anterior WML score	0.9±0.8	1.4±0.9	**0.03**	**2.23 (1.05 to 4.74)**	**2.84 (1.22 to 6.60)**
Posterior WML score	0.7±0.8	1.4±0.9	**0.01**	**2.44 (1.24 to 4.81)**	**3.56 (1.60 to 7.91)**
Total WML score	1.6±1.5	2.8±1.7	**0.02**	**1.61 (1.11 to 2.35)**	**1.99 (1.27 to 3.12)**
Prominent juxtacortical WML	47 (16.4%)	9 (69.2%)	**<0.001**	**10.6 (3.31 to 34.3)**	**20.9 (4.94 to 88.6)**
Pattern 1	26 (55.3%)	4 (44.4%)	0.72		
Pattern 2	21 (44.7%)	5 (55.6%)			
Anterior temporal lobe WML	1 (0.35%)	0 (0%)	0.83	NA	NA
External capsule WML	33 (11.5%)	6 (46.2%)	**<0.001**	**6.56 (2.14 to 20.1)**	**8.28 (2.27 to 30.2)**
Cortical atrophy score	0.7±0.7	1.0±0.8	0.24	1.56 (0.77 to 3.17)	1.85 (0.69 to 4.96)
Central atrophy score	0.9±0.8	1.2±1.0	0.25	1.51 (0.79 to 2.91)	1.75 (0.74 to 4.14)
Total atrophy score	1.6±1.5	2.2±1.7	0.23	1.28 (0.89 to 1.83)	1.44 (0.87 to 2.41)
Presence of lacune	125 (43.7%)	8 (61.5%)	0.26	1.99 (0.66 to 5.98)	2.15 (0.72 to 6.42)
Number of lacune	1.2±1.9	1.9±2.1	0.13	1.18 (0.95 to 1.47)	1.21 (0.96 to 1.51)
Prominent lobar lacune	25 (8.7%)	3 (23.1%)	0.11	3.42 (0.94 to 12.5)	**3.91 (1.03 to 14.8)**

Numbers in bold indicating statistical significance (P<0.05).
*Adjusted by age, sex and hyperlipidaemia.
WML, white matter lesion.

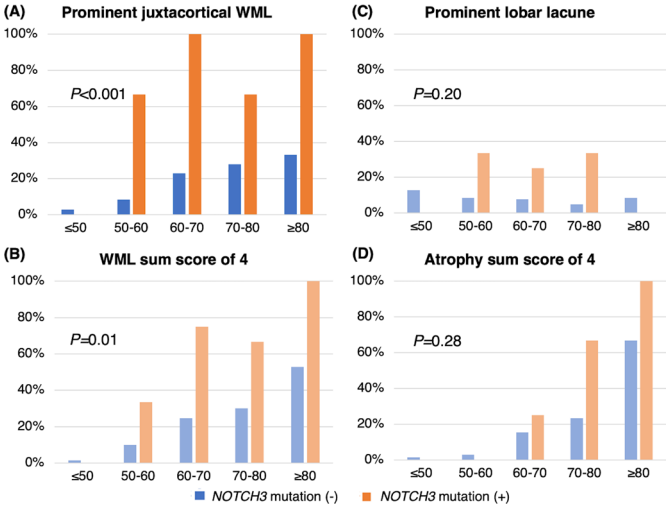

Figure 3 The presence of CT features across different age groups between patients with and without *NOTCH3* p.R544C mutation. (A) Prominent juxtacortical white matter lesion (WML), (B) maximum WML score, (C) prominent lobar lacune and (D) maximum cerebral atrophy score. P value was derived from the Cochrane-Mantel-Haenszel test.

1.2±1.9, p=0.13) and a higher frequency of prominent lobar lacunes (23% vs 9%, p=0.11).

If stratified by the age group, the frequency of prominent juxtacortical WML exceeded 50% in patients with *NOTCH3* p.R544C mutation who were aged >50 years, whereas the frequency increased gradually with age but was still <50% in patients without *NOTCH3* p.R544C mutation (p<0.001; Cochrane-Mantel-Haenszel test; figure 3A). Furthermore, the distribution of the WML sum score of 4, which represents the most severe and diffuse WML, was statistically significant across age groups between the two groups (p=0.01; figure 3B). The distribution of prominent lobar lacunes or maximum cerebral atrophy score was comparable between the two groups (figure 3C–D).

In multivariable analysis after adjusting for age, sex and hyperlipidemia, CT features independently associated with *NOTCH3* p.R544C mutation included the total WML score (OR, 1.99; 95% CI 1.27 to 3.12), prominent juxtacortical WML (OR, 20.9; 95% CI 4.94 to 88.6), external capsule WML (OR 8.28; 95% CI 2.27 to 30.2) and prominent lobar lacunes (OR, 3.91; 95% CI 1.03 to 14.8; table 2). When the aforementioned CT features

Table 3 Performance of clinical and CT features in predicting *NOTCH3* p.R544C mutation

	aOR (95% CI)*	AUC-ROC (95% CI)	P value †
Total WML score	0.79 (0.37 to 1.66)	0.69 (0.52 to 0.86)	**0.047**
External capsule WML	1.70 (0.39 to 7.33)	0.67 (0.53 to 0.82)	0.141
Prominent lobar lacune	2.32 (0.53 to 10.13)	0.57 (0.45 to 0.69)	**0.038**
Prominent juxtacortical WML	20.4 (1.54 to 271.0)	0.76 (0.63 to 0.90)	–

Numbers in bold indicating statistical significance (P<0.05).
*Simultaneously adjusted with these three imaging markers.
†Compared with prominent juxtacortical WML alone.
aOR, adjusted OR; AUC-ROC, area under the receive operating characteristic curve; WML, white matter lesion.

were mutually adjusted, the neuroimaging features most significantly associated with *NOTCH3* p.R544C mutation was prominent juxtacortical WML (OR, 20.4; 95% CI 1.54 to 271.0; table 3). In the receiver operative characteristics analysis, prominent juxtacortical WML (AUC, 0.76; 95% CI 0.63 to 0.90) outperformed the total WML score (AUC, 0.69; 95% CI 0.52 to 0.86; p=0.047) and prominent lobar lacunes (AUC, 0.57; 95% CI 0.45 to 0.69; p=0.038) and was also numerically higher than external capsule WML (AUC, 0.67; 95% CI 0.53 to 0.82).

Overall, the sensitivity, specificity, positive predictive value, negative predictive value and diagnostic accuracy of using prominent juxtacortical WML for predicting *NOTCH3* p.R544C mutation were 69.2%, 83.6%, 16.1%, 98.4% and 82.9%, respectively. In patients with *NOTCH3* p.R544C mutation, those with prominent juxtacortical WML (n=9) had a higher WML score, higher cerebral atrophy score, more external capsule WML involvement and more lacunes than did those without prominent juxtacortical WML (n=4; table 4). When comparing patients with prominent juxtacortical WML with and without (n=47) *NOTCH3* p.R544C mutation, the severity of WML, cerebral atrophy and lacunes were similar between the two groups.

Table 4 Comparison between patients with *NOTCH3* p.R544C mutation with and without prominent juxtacortical white matter lesion

	***NOTCH3* mutation, juxtacortical WML (+)**	***NOTCH3* mutation, juxtacortical WML (–)**	**Non-mutation, juxtacortical WML (+)**
Number	9	4	47
Age	67.3±10.1	57.3±14.6	71.8±11.7
Male sex	6 (66.7%)	2 (50.0%)	32 (68.1%)
ICH location			
Thalamus	4 (44.4%)	2 (50.0%)	19 (40.4%)
Basal ganglia	2 (22.2%)	1 (25.0%)	8 (17.0%)
Cortical-subcortical	1 (11.1%)	0 (0.0%)	11 (23.4%)
Infratentorium	2 (22.2%)	1 (25.0%)	9 (19.1%)
ICH size, mL	13.4±17.7	13.4±21.3	13.0±17.5
IVH	3 (33.3%)	1 (25.0%)	21 (44.7%)
CT features			
Anterior WML score	1.9±0.3	0.3±0.5	1.9±0.3
Posterior WML score	1.9±0.3	0.3±0.5	1.9±0.3
Total WML score	3.8±0.4	0.5±1.0	3.8±0.5
Anterior temporal lobe WML	0 (0%)	0 (0%)	1 (2.1%)
External capsule WML	6 (66.7%)	0 (0%)	21 (44.7%)
Cortical atrophy score	1.2±0.8	0.5±0.6	1.2±0.7
Central atrophy score	1.4±0.9	0.5±1.0	1.6±0.6
Total atrophy score	2.7±1.7	1.0±1.4	2.9±1.1
Presence of lacune	7 (77.8%)	1 (25.0%)	30 (63.8%)
Number of lacune	2.7±2.2	0.3±0.5	2.3±2.8
Prominent lobar lacune	2 (22.2%)	1 (25.0%)	8 (17.0%)

ICH, intracerebral haemorrhage; IVH, intraventricular haemorrhage; WML, white matter lesion.

Table 5 Comparison of the neuroimaging features between patients who had received both the CT and MRI scans

N=145	CT	MRI	Kappa values (95% CI)
Anterior WML≥2	46 (31.7%)	60 (41.4%)	0.74 (0.62 to 0.85)
Posterior WML ≥2	43 (29.7%)	67 (46.2%)	0.63 (0.51 to 0.75)
Prominent juxtacortical WML	33 (22.9%)	44 (30.6%)	0.81 (0.70 to 0.91)
Anterior temporal lobe WML	0 (0%)	1 (0.7%)	0.66 (0.04 to 1.00)
External capsule WML	23 (16.0%)	22 (15.3%)	0.97 (0.92 to 1.00)
Presence of lacune	70 (48.6%)	76 (52.8%)	0.81 (0.71 to 0.90)

WML, white matter lesion.

In addition, 145 of the 299 patients had received a follow-up MRI study. The median intervals between the CT and MRI studies were 3 days. Of them, eight were known to have *NOTCH3* p.R544C mutation. The Kappa values were good (0.63 to 0.74) for the presence of severe anterior and posterior WML and anterior temporal lobe WML and were excellent (0.81 to 0.97) for the presence of prominent juxtacortical WML, external capsule WML and lacunes (table 5).

DISCUSSION

The results of the present study showed that when using non-contrast CT images in patients with spontaneous ICH, the presence of a prominent juxtacortical WML hallmarks the possibility of an underlying *NOTCH3* p.R544C mutation. Other features closely associated with *NOTCH3* p.R544C mutation included a high WML score and prominent lobar lacune. Although MRI remains the standard neuroimaging technique for evaluating SVD, CT is usually the first-line study especially when encountering ICH. Therefore, our findings may facilitate primary care physicians in identifying the potential genetic cause of SVD and arranging appropriate referral to the specialist. In addition, although these CT features may also be presented in the older population, the predominant presentation in rather young patients argued for an underlying hereditary SVD.

Hypertensive-related SVD is the major cause of spontaneous ICH in adults. All patients with *NOTCH3* p.R544C mutation in this study had hypertension, and the location and size of ICH were also indistinguishable from those in patients without mutations. The thalamus was the most common location of ICH and cerebral microbleeds in patients with CADASIL.[6 16] However, in the present study, the difference in the proportions of thalamic ICH was not statistically significant. Collectively, ICH features themselves could not provide sufficient diagnostic clues.

In patients with *NOTCH3* p.R544C mutation, WML severity was significantly high, which was not surprising because CADASIL is notable for its leucoencephalopathy. In addition to the visual analysis of WML, a prominent juxtacortical WML could provide clues in distinguishing patients with *NOTCH3* p.R544C mutation from those without. In clinical practice, prominent juxtacortical WML can be seen in ageing patients and those with multiple sclerosis, cerebral SVD, leucodystrophy and history of receiving whole brain irradiation. Periventricular WML may be more haemodynamically relevant, while deep or subcortical WML is attributed to SVD.[17] Even in patients with hypertension, combining the presence of ICH and a prominent juxtacortical WML suggest a profound underlying SVD load, in which a hereditary cause should be considered. Given the low prevalence of *NOTCH3* p.R544C mutation among patients with spontaneous ICH, using prominent juxtacortical WML alone may reveal the positive predictive value to be considerably low, and false negative may emerge. Many patients without *NOTCH3* p.R544C mutation may still present with a prominent juxtacortical WML, especially when they are older and have advanced SVD (figure 2A). Interestingly, our study showed that in patients with ICH and *NOTCH3* p.R544C mutation, the prevalence of prominent juxtacortical WML was more than half irrespective of their age. In other words, in relatively younger patients (ie, those aged <70 years), the presence of this sign on CT could be seen as a first-line screening tool to guide clinicians for further referral, especially if head MRI is not readily available. Nonetheless, defined two patterns of prominent juxtacortical WML, they seemed non-correlated with the status of *NOTCH3* p.R544C mutation, which implied that both patterns of prominent juxtacortical WML, if present, have similar clinical significance.

The characteristic WML involvement in the anterior temporal lobe (O'Sullivan's sign) and external capsule area in patients with CADASIL might be more easily seen on the MRI scan rather than CT.[18] In our study, anterior temporal lobe hypodensity on CT was rarely seen. The reason for such a low prevalence may be attributed to the low detection rate by non-contrast CT scan. However, even by the MRI, our recent study suggested that the anterior temporal lobe involvement was only presented in 22% of the patients with *NOTCH3* p.R544C mutation.[19] Therefore, using anterior temporal lobe hypodensity by CT scan is not ideal for diagnosis. On the other hand, the presence of external capsule hypodensity was around 46% in patients with *NOTCH3* p.R544C mutation, compared with 12% in patients without the mutation. However, when mutually adjusted with other neuroimaging features, prominent juxtacortical WML still outperformed external capsule WML in predicting *NOTCH3*

p.R544C mutation. Besides, it should be noted that the interpretation of hypodensity in the external capsule area may be interfered by nearby dilated perivascular space or old insults, which may limit its clinical usefulness.

In addition to WML, we found that the number of lacunes and prominent lobar lacunes was borderline significantly associated with *NOTCH3* p.R544C mutation. A high number of lacunes possibly reflected a high background SVD load in patients with *NOTCH3* mutation. Interestingly, according to two recent MRI-based studies, the prominent lobar lacune was more frequently found in cerebral amyloid angiopathy-related ICH than in hypertensive ICH.[20 21] Nonetheless, the prevalence of lobar lacunes was still approximately 5.8%–11.6% in hypertensive ICH in these studies. Our CT-based study found that the prominent lobar lacune can be seen in nearly one-fourth of patients with *NOTCH3* p.R544C mutation. These findings suggest that not only number of lacunes but also its topographic distribution is suggestive of different underlying mechanisms. Additional studies, possibly using MRI, to elucidate the pathophysiology of lobar lacunes in patients with CADASIL are strongly warranted.

The prevalence of hyperlipidemia was found to be twofold higher in patients with *NOTCH3* p.R544C mutation (69.2% vs 31.1%). Observational studies and meta-analysis have suggested that the total cholesterol and low-density lipoprotein levels were inversely associated with the risk of ICH, and high-intensity statin used in the clinical trials was also linked with the occurrence of haemorrhagic stroke.[22 23] One of the limitations of our study is that we did not collect information on statin use and the cholesterol level at the index ICH event. We retrospectively evaluated nine patients with *NOTCH3* p.544C mutation and hyperlipidemia and found that none of them was under statin use. One possibility was that the high cholesterol level in these patients was reflective of their advanced vascular burden. Nonetheless, the effects of dyslipidaemia on the progression and neuroimaging markers of SVD remained ambiguous and need further investigation.

Recently, a clinical and MRI-based pregenetic screening score was developed to efficiently identify patients with acute ischaemic stroke who may harbour an *NOTCH3* p.R544C mutation.[19] Our present study was unable to derive a similar score owing to relatively small sample sizes. These studies only screened p.R544C mutation given its relatively high prevalence in Taiwan; thus, the findings may not be generalised to areas where *NOTCH3* p.R544C is not the predominant mutation. Additionally, even in Taiwan, approximately 30% of patients with CADASIL had *NOTCH3* mutations other than p.R544C,[8] hence, the absence of p.R544C does not rule out the possibility of hereditary SVD. Another major limitation is that MRI was not performed routinely in the present cohort; therefore, we did not have the information regarding the number and location of cerebral microbleeds. However, based on available MRI in our study population, the consistency of interpretating neuroimaging features of SVD between CT and MRI was excellent. Since CT is the most commonly performed neuroimaging technique in patients with acute ICH, a CT-based screening feature still has its value.

Limitations and pitfalls of using CT to evaluate SVD markers should be acknowledged. For example, the evaluation of juxtacortical WML might have been affected by the following factors. First, if patients had severe hydrocephalus and transependymal absorption, the WML extent was often exaggerated. Second, when the patient had prior ventricular drainage or surgical process involving the high frontal lobe, the white matter may become hypodense and even mimic juxtacortical WML. In such a situation, the interpretation must be scrutinised. Additionally, the detection rate of lacunes on CT is lower than that on MRI because of poorer tissue contrast. In few of our patients, only axial view images were available, which may further lower the detection rate of lacunes.

In summary, in patients with spontaneous ICH in Taiwan, patients carrying *NOTCH3* p.R544C mutation had more severe WML compared with non-carriers. A prominent juxtacortical distribution of WML, especially in rather young patients, was highly suggestive of *NOTCH3* p.R544C mutation-related ICH.

Acknowledgements This manuscript was edited by Wallce Academic Editing.

Contributors C-HC acquired and analysed the data and drafted the manuscript. H-CH acquired and analysed the data. Y-WC acquired and analysed the data. Y-FC designed the study, arranged the neuroimaging, acquired and analysed the data, and critically revised the manuscript. S-CT designed the study and critically revised the manuscript. J-SJ supervised the study and critically revised the manuscript.

Funding The authors have not declared a specific grant for this research from any funding agency in the public, commercial or not-for-profit sectors.

Competing interests None declared.

Patient consent for publication Not required.

Ethics approval This study was approved by the research ethics committees of National Taiwan University Hospital NTUH REC-No. 201810003RIND.

Provenance and peer review Not commissioned; externally peer reviewed.

Data availability statement Data are available upon reasonable request.

ORCID iD

Chih-Hao Chen http://orcid.org/0000-0002-1258-8775

REFERENCES

1 Ziai WC, Carhuapoma JR. Intracerebral hemorrhage. *Continuum* 2018;24:1603–22.
2 Yeh S-J, Tang S-C, Tsai L-K, *et al*. Pathogenetical subtypes of recurrent intracerebral hemorrhage: designations by SMASH-U classification system. *Stroke* 2014;45:2636–42.
3 Pantoni L. Cerebral small vessel disease: from pathogenesis and clinical characteristics to therapeutic challenges. *Lancet Neurol* 2010;9:689–701.
4 Choi JC. Genetics of cerebral small vessel disease. *J Stroke* 2015;17:7–16.
5 Chabriat H, Joutel A, Dichgans M, *et al*. Cadasil. *Lancet Neurol* 2009;8:643–53.

6 Chen C-H, Tang S-C, Cheng Y-W, *et al*. Detrimental effects of intracerebral haemorrhage on patients with CADASIL harbouring Notch3 R544C mutation. *J Neurol Neurosurg Psychiatry* 2019;90:841–3.
7 Choi JC, Kang S-Y, Kang J-H, *et al*. Intracerebral hemorrhages in CADASIL. *Neurology* 2006;67:2042–4.
8 Liao Y-C, Hsiao C-T, Fuh J-L, *et al*. Characterization of CADASIL among the Han Chinese in Taiwan: distinct genotypic and phenotypic profiles. *PLoS One* 2015;10:e0136501.
9 Choi JC, Song S-K, Lee JS, *et al*. Diversity of stroke presentation in CADASIL: study from patients harboring the predominant NOTCH3 mutation R544C. *J Stroke Cerebrovasc Dis* 2013;22:126–31.
10 Tang S-C, Chen Y-R, Chi N-F, *et al*. Prevalence and clinical characteristics of stroke patients with p.R544C *NOTCH3* mutation in Taiwan. *Ann Clin Transl Neurol* 2019;6:121–8.
11 Hemphill JC, Bonovich DC, Besmertis L, *et al*. The ICH score: a simple, reliable grading scale for intracerebral hemorrhage. *Stroke* 2001;32:891–7.
12 Kothari RU, Brott T, Broderick JP, *et al*. The ABCs of measuring intracerebral hemorrhage volumes. *Stroke* 1996;27:1304–5.
13 van Swieten JC, Hijdra A, Koudstaal PJ, *et al*. Grading white matter lesions on CT and MRI: a simple scale. *J Neurol Neurosurg Psychiatry* 1990;53:1080–3.
14 Sato S, Delcourt C, Heeley E, *et al*. Significance of cerebral small-vessel disease in acute intracerebral hemorrhage. *Stroke* 2016;47:701–7.
15 Anderson JA, Blair V. Penalized maximum likelihood estimation in logistic regression and discrimination. *Biometrika* 1982;69:123–36.
16 Chung C-P, Chen J-W, Chang F-C, *et al*. Cerebral microbleed burdens in specific brain regions are associated with disease severity of cerebral autosomal dominant arteriopathy with subcortical infarcts and leukoencephalopathy. *J Am Heart Assoc* 2020;9:e016233.
17 Kim KW, MacFall JR, Payne ME. Classification of white matter lesions on magnetic resonance imaging in elderly persons. *Biol Psychiatry* 2008;64:273–80.
18 O'Sullivan M, Jarosz JM, Martin RJ, *et al*. MRI hyperintensities of the temporal lobe and external capsule in patients with CADASIL. *Neurology* 2001;56:628–34.
19 Cheng Y-W, Chen C-H, Hu C-J, *et al*. Imaging-based pregenetic screening for NOTCH3 p.R544C mutation in ischemic stroke in Taiwan. *Ann Clin Transl Neurol* 2020;7:1951–61.
20 Pasi M, Boulouis G, Fotiadis P, *et al*. Distribution of lacunes in cerebral amyloid angiopathy and hypertensive small vessel disease. *Neurology* 2017;88:2162–8.
21 Tsai H-H, Pasi M, Tsai L-K, *et al*. Distribution of lacunar infarcts in Asians with intracerebral hemorrhage: a magnetic resonance imaging and amyloid positron emission tomography study. *Stroke* 2018;49:1515–7.
22 Wang X, Dong Y, Qi X. Cholesterol levels and risk of hemorrhagic stroke: a systematic review and meta-analysis. *Stroke* 2013;44:1833–9.
23 Amarenco P, Bogousslavsky J, Callahan A, *et al*. High-dose atorvastatin after stroke or transient ischemic attack. *N Engl J Med* 2006;355:1374–59.